

**Quick Search** All fields  Author   
 ? search tips Journal/book title  Volume  Issue  Page  CI

**Materials Chemistry and Physics**

Volume 113, Issues 2-3, 15 February 2009, Pages 702-706

 Font Size:  
**Article**
[Figures/Tables](#)
[References](#)
 PDF (916 K)



[Thumbnails](#) | [Full-Size Images](#)

doi:10.1016/j.matchemphys.2008.07.131

? Cite or Link Using DOI

Copyright © 2008 Elsevier B.V. All rights reserved.

## Growth and characterization of BLZT–CFO composite thin films

 E. Delgado<sup>a, b, c</sup>, C. Ostos<sup>b</sup>, , , M.L. Martínez-Sarrión<sup>b</sup>, L. Mestres<sup>b</sup>, D. Lederman<sup>c</sup> and P. Prieto<sup>d</sup>
<sup>a</sup>Department of Physics, Universidad del Valle, Building 320-3001, Cali, Colombia

<sup>b</sup>Department of Inorganic Chemistry, University of Barcelona, C/Martí i Franquès, 1-11, 08028, Barcelona, Spain

<sup>c</sup>Department of Physics, West Virginia University, Morgantown, WV 26506, USA










<sup>d</sup>Excellence Centre for Novel Materials, Universidad del Valle, A.A. 25360, Cali, Colombia

Received 19 March 2008; revised 16 July 2008; accepted 24 July 2008. Available online 23 September 2008.

**Abstract**

 Composite Ba<sub>0.90</sub>La<sub>0.067</sub>Zr<sub>0.09</sub>Ti<sub>0.91</sub>O<sub>3</sub>–CoFe<sub>2</sub>O<sub>4</sub> (BLZT–CFO) thin films were prepared

**Article Toolbox**






-  Download PDF
-  Export Citation
-  E-mail Article
-  Add to my Quick Links
-  Cited By
-  Add to **collab**
-  Save as Citation Alert
-  Permissions & Reprints
-  Citation Feed

**Related Articles in ScienceDirect**

- [Electric and magnetic properties of Pb\(Zr<sub>0.52</sub>Ti<sub>0.48</sub>\)O<sub>3</sub>...](#)  
*Materials Research Bulletin*
- [Structure and properties of Ti-C-B composite thin films...](#)  
*Surface and Coatings Technology*
- [Structural, electrical and magnetic properties of carbo...](#)  
*Carbon*
- [Flower-like Pb\(Zr<sub>0.52</sub>Ti<sub>0.48</sub>\)O<sub>3</sub> nanoparticles on the CoF...](#)  
*Journal of Crystal Growth*
- [Cobalt/Polymer Composite Thin Films](#)  
*Ultra-Fine Particles*

[View More Related Articles](#)

**The research collaboration tool**


-   No user rating
-  No user tags yet
-  This article has not yet been bookmarked
-  No comments on this article yet
-  Not yet shared with any groups

 Be the first to add this article in **collab**

by rf-magnetron sputtering from a 0.68 BLZT–0.32 CFO mixed target at a substrate temperature of 1033 K in a high oxygen pressure atmosphere. Single-crystal conducting Nb-doped (1%) SrTiO<sub>3</sub> and Pt-coated Si substrates were used. X-ray diffraction (XRD) patterns revealed that the films had both BLZT and CFO phases. Scanning electron microscopy (SEM) showed that the CFO phase was intermixed into a BLZT matrix. X-ray photoelectron spectroscopy (XPS) data in depth profile mode showed that all constituent elements were present and confirmed the favourable TiO<sub>6</sub>-octahedron distortion in the BLZT-perovskite structure. The Au/BLZT–CFO/substrate capacitors were ferroelectric and magnetic at room temperature. The magnetoelectric nature of the composite thin films was demonstrated through the reduction of measured ferroelectric polarization with the application of an external magnetic field.

**Keywords:** Thin films; Composite materials; Magnetron sputtering

## Article Outline

1. [Introduction](#)
2. [Experimental](#)
3. [Results and discussion](#)
4. [Conclusions](#)

[Acknowledgements](#)

[References](#)

## 1. Introduction

Ferroelectric materials are attractive candidates for the next generation of non-volatile memories (FRAM), given unique properties, such as spontaneous polarization, low operating voltage and high fatigue resistance [1], [2], [3] and [4]. In the development of high-density ferroelectric memories, density must be increased by reducing both lateral and thickness dimensions occupied by a memory capacitor. At the same time, measurable and stable ferroelectric properties must also be maintained [5]. Two families of these materials, lead zirconate titanate (PZT) and strontium bismuth tantalate (SBT), have been investigated widely for memory applications [6]. Other ferroelectric lead-free

materials of the same family have emerged, such as barium lanthanide zirconate titanate (BLnZT; Ln = La, Nd) compounds, which have very high dielectric constants and good ferroelectric response [7] and [8]. In terms of recent advances in magnetic materials, the potential impact on society is extensive. Some examples, such as dramatic increases in data storage density are already evident [9]. The discoveries of giant and colossal magneto-resistive materials, where magnetic fields cause order of magnitude changes in conductivity, have been particularly significant. Sensors, read heads, and memories based on giant magneto-resistive [10], [11] and [12] magnetic multilayers [13], [14] and [15] are already commercially available.

In this paper, we explore the BLZT–CFO multiferroic composite. Multiferroic materials [16] and [17] display simultaneous electric and magnetic ordering and a coupling exists between the ferroelectric and magnetic polarizations. A whole range of new applications can be envisaged given additional degrees of freedom in device design. The BLZT–CFO composite thin films were deposited by rf-magnetron sputtering from a  $\text{Ba}_{0.90}\text{La}_{0.067}\text{Zr}_{0.09}\text{Ti}_{0.91}\text{O}_3\text{--CoFe}_2\text{O}_4$  mixed target. The films were grown on Nb-doped  $\text{SrTiO}_3$ , which is electrically conducting and considered an adequate substrate for the preparation of epitaxial films [18] and [19], and on  $\text{Pt/TiO}_2/\text{SiO}_2/\text{Si}$  [20] substrates, which is a common bottom-electrode for the fabrication of capacitor devices. Emphasis was placed on the structural, morphological and chemical characterization and on how magnetic properties influence the ferroelectric properties of BLZT–CFO thin films.

## 2. Experimental

BLZT–CFO composite thin films were prepared on single-crystal Nb-doped  $\text{SrTiO}_3$  (1 0 0) – Nb:STO– and  $\text{Pt}(1\ 1\ 1)/\text{TiO}_2/\text{SiO}_2/\text{Si}$  –Pt– substrates by rf-magnetron sputtering in a high pressure-oxygen atmosphere. Deposition conditions for the multiferroic were tuned by optimizing the condition to obtain a good epitaxial film, as shown in Table 1.

Table 1.

Growth conditions of BLZT–CFO composite thin films by rf-magnetron sputtering

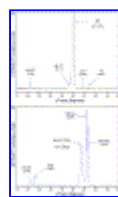
| Sputtering parameters     | Conditions   |
|---------------------------|--|
| Target                    | Ba <sub>0.90</sub> La <sub>0.067</sub> Zr <sub>0.09</sub> Ti |
| Substrates                | Nb:STO; Pt   |
| Target-substrate distance | 28 mm  |
| Atmosphere                | O <sub>2</sub>   |
| Vacuum pressure           | 2.7 × 10 <sup>-4</sup> Pa                                    |
| Work pressure             | 1.2 × 10 <sup>4</sup> Pa                                     |
| Deposition time           | 10–60 min  |
| RF power                  | 60 W   |
| BIAS                      | 400–650 volts  |
| Substrate temperature     | 1033 K   |

The target was synthesized by mixing of 68% (by mass) Ba<sub>0.90</sub>La<sub>0.067</sub>Zr<sub>0.09</sub>Ti<sub>0.91</sub>O<sub>3</sub> pure perovskite-type compound obtained from oxalate-peroxide method [21], and 32% CoFe<sub>2</sub>O<sub>4</sub> pure spinel-type compound obtained from solid-state reaction. The films grown were structurally characterized via X-ray diffraction (XRD) using a Phillips MRD diffractometer with parallel optical beam, Cu K $\alpha$  radiation and a Bartel-type monochromator. Film surface roughness and morphology were examined by atomic force microscopy (AFM) in a Veeco Metrology Group microscope and by scanning electron microscopy (SEM) in a LEICA Cambridge S360 microscope with a Steroscan 260 EDX analyzer. X-ray photoelectron spectroscopy (XPS) analysis of the surface was performed in a Perkin Elmer PHI 5500–ESCA System. The analysis was done in depth profile mode and the sputter was achieved using a Ar<sup>+</sup> ion gun with accelerating voltage of 4 keV and emission current of 15 mA. The ferroelectric polarization and leakage current density of a Au/BLZT–CFO/substrate capacitor were measured at room temperature using a Precision LC Radiant Technologies ferroelectric measurement system. The round gold top electrodes had an area of 6.5 × 10<sup>-3</sup> cm<sup>2</sup> and

were deposited by thermal evaporation using a shadow mask. The magnetic properties of the composite thin film were measured using a superconducting quantum interference device (SQUID) magnetometer. A linear diamagnetic background was subtracted from the magnetization measured as a function of magnetic field.

### 3. Results and discussion

Several thin films obtained from a pure composite target were evaluated by XRD measurements. The diffraction peaks were identified as reflections of the barium zirconate titanate perovskite (JCPDS 36-0019) and spinel cobalt ferrite (JCPDS 22-1086). As a representative sample, Fig. 1 shows the XRD  $\theta$ - $2\theta$  scans of composite thin films grown on (a) conducting Pt and (b) single-crystal Nb:STO substrates.



[Full-size image \(47K\)](#)

Fig. 1. XRD patterns of BLZT-CFO composite deposited on (a) Pt and (b) single-crystal Nb:STO substrates.

For samples deposited on Pt (Fig. 1a), the BLZT showed initial  $\langle 111 \rangle$ -oriented growth along the  $[111]$ -direction of the platinum film, perpendicular to the sample's surface. After 30 min of deposition the perovskite  $(100)$ -peak was observed, which is parallel to the  $c$ -axis direction. The  $(400)$ -crystal plane of the spinel cobalt ferrite could not be clearly observed until the perovskite growth was started, and no additional peaks were detected showing a  $\langle 00 \rangle$ -crystal growth. For the composite thin films deposited on Nb:STO (Fig. 1b), growth along the  $\langle 001 \rangle$ -direction was observed. However, the CFO  $(400)$ -crystal plane overlapped with BLZT  $(200)$ -peak and therefore

it was not possible to distinguish between them. Furthermore, films deposited on Nb:STO substrate have better crystallinity due to the similar lattice parameters (3.899 Å) and same perovskite-type structure with respect to the first layers deposited.

The surface morphology of crystallized BLZT–CFO thin films was analyzed by AFM (Fig. 2). The scan area of analysis was  $3 \times 3 \mu\text{m}^2$ .

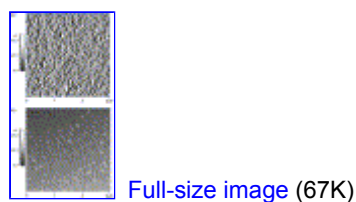


Fig. 2. AFM image of BLZT–CFO grown on (a) Pt and (b) Nb:STO substrates for 30 min of deposition.

Film growth on Pt (Fig. 2a) revealed grains without clear grain boundaries on the surface, which implies that many grains coalesced due to high-temperature thermal annealing. Film growth on this substrate was confirmed with a root-mean-square (RMS) roughness value of 5.06 nm. Thin film deposited on Nb:STO (Fig. 2b) showed a softer texture with an RMS roughness value of 3.54 nm. The image shows spherical grains with well-defined boundaries, from which the average size particle was determined to be approximately 156 nm.

The SEM micrograph on BLZT–CFO/Pt depicted in Fig. 3a shows that the phase in black is evenly and randomly embedded in the grey matrix. The EDS analysis on the composite thin film (Fig. 3b) revealed strong Ba and Ti peaks with minor of Co and Fe peaks. The results suggest that the major composition of the matrix is the BLZT deposited compound. The black dots were identified as  $\text{CoFe}_2\text{O}_4$  rich zones since EDS spot scan analyses of those areas exhibit stronger Co and Fe peaks than in the grey areas. The incident electron beam penetrated several micrometers

deep into the sample, which prevents a unique single-phase EDS spectrum and results in the appearance of other peaks, such as those corresponding to platinum and silicon from the substrate. Moreover, the diameter of the electron beam was approximately 1  $\mu\text{m}$ , and therefore additional background peaks were observed since the CFO regions in the BLZT matrix were approximately 0.5  $\mu\text{m}$  wide.

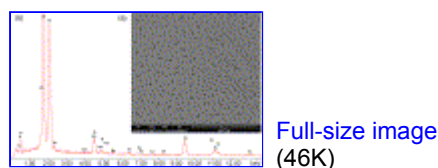
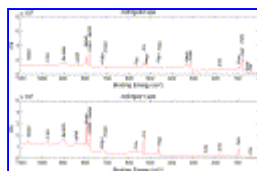


Fig. 3. (a) Typical SEM micrograph of BLZT–CFO thin film on Pt substrate. Black dots detected by (b) EDS spectrum correspond to Co- and Fe-rich zones (black dots) embedded in the BLZT matrix (grey zone).

A similar analysis of the BLZT–CFO/STO system was not possible due to the strong titanium peak from STO substrate which was in the same energy range as the peaks from the samples. In any case, the EDS spectrum did show Co- and Fe-peaks.

To determine the effective presence of each constituent element in the films, XPS measurements were performed in depth profile by etching samples with argon ions. The analysis was conducted in samples deposited on the Pt substrate in order to avoid titanium interferences from Nb:STO substrate. This allowed for accurate element analysis, the possibility of calculating the thickness of the thin film, and a chemical-environment analysis of titanium of  $\text{TiO}_6$ -octahedron in the perovskite structure. Fig. 4 shows XPS survey spectra of a composite thin film that was sputter-cleaned with 4 keV  $\text{Ar}^+$  ions.

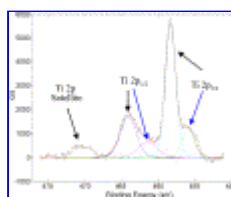


Full-size image  
(51K)

Fig. 4. XPS survey spectra of BLZT–CFO film grown on Pt etched during (a) 1 min and (b) 5 min.

The analysis for 1 min etching time shows the absence of platinum binding energy peaks on the substrate. The film etched for 5 min allowed an average depth of analysis of 100 nm. The XPS spectra at this time revealed the presence of platinum for the film deposited for 30 min, which is equivalent to a growth rate of between  $2 \text{ nm min}^{-1}$  and  $3 \text{ nm min}^{-1}$ . The presence of each element from the ferroelectric (Ba, La, Ti, Zr) and magnetic (Co, Fe) compounds was confirmed throughout the film by the peaks with the following photoelectron binding energies: La  $3d_{3/2} = 851.2 \text{ eV}$  and La  $3d_{5/2} = 833.7 \text{ eV}$ ; Zr  $3d = 179.26 \text{ eV}$ ; Ba  $3d_{5/2} = 780.35 \text{ eV}$  and Ba  $3d_{3/2} = 795.55 \text{ eV}$  overlapping Co  $2p_{3/2}$  and Co  $2p_{1/2}$ , respectively; Fe  $2p_{3/2} = 709.18 \text{ eV}$  and Fe  $2p_{1/2} = 722.97 \text{ eV}$ . The Ti  $2p_{3/2}$  and Ti  $2p_{1/2}$  signals are discussed later.

Possible structural modifications of the structure were identified from modifications of the binding energy of the titanium peaks. A possible distortion of  $\text{TiO}_6$ -octahedron in the perovskite structure could result from the intrinsic ferroelectric structure or from extrinsic modifications originating from the alloying with zirconium and lanthanum. Fig. 5 shows the fitted-narrow scan spectrum of Ti 2p doublets in the composite thin film.

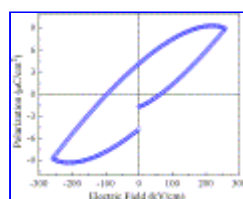


Full-size image (35K)

Fig. 5. Ti 2p photoelectron spectrum of the BLZT–CFO composite deposited on Pt.

The scan confirmed typical barium titanate signals at 464.06 eV for Ti 2p<sub>1/2</sub> and 458.32 eV for Ti 2p<sub>3/2</sub> ( $\Delta E = 5.74$  eV), and a second doublet at lower energies at 461.65 eV for Ti 2p<sub>1/2</sub> and 455.94 eV for Ti 2p<sub>3/2</sub> ( $\Delta E = 5.71$  eV). The signal at 471.0 eV corresponds to the Ti 2p shake-up satellite peak. These results confirm the TiO<sub>6</sub><sup>-</sup> octahedron distortion and we can thus predict a possible enhancement of the ferroelectric properties in BLZT–CFO composite thin films, when compared to a similar BaTiO<sub>3</sub>/CoFe<sub>2</sub>O<sub>4</sub> system.

The BLZT–CFO composite thin film exhibited ferroelectric and magnetic properties at room temperature. The composite film shows a well-defined ferroelectric loop, as shown in Fig. 6.



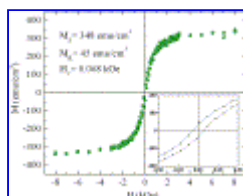
Full-size image (35K)

Fig. 6. Polarization hysteresis loop of the composite film measured at room temperature.

The remanent polarization ( $P_r$ ) and coercive field ( $E_c$ ) values were approximately  $4.2 \mu\text{C cm}^{-2}$  and  $65.1 \text{ kV cm}^{-1}$ , respectively. The  $P_r$  and  $E_c$  for pure BLZT thin films has been measured to be  $8.5 \mu\text{C cm}^{-2}$  and  $53.6 \text{ kV cm}^{-1}$ , respectively [7]. The smaller value of  $P_r$  in the composite film could be due to the presence of non-ferroelectric CFO regions which may also hinder ferroelectric domain wall motion, thus resulting in the larger  $E_c$  of the composite film. An analysis of the leakage current density was used to make sure that the hysteresis loops were not due to leakage through the film.

The magnetization dependence on the magnetic

field was measured at room temperature by applying a magnetic field up to 8 KOe. Fig. 7 shows the magnetic hysteresis loop for the BLZT–CFO composite film.

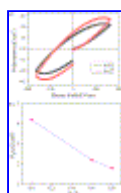


Full-size image (37K)

Fig. 7. In-plane magnetization *versus* magnetic field curve of the sample measured at room temperature. Inset: same data for small fields.

The saturation magnetization ( $M_s$   $\sim 348$  emu cm $^{-3}$ ) of BLZT–CFO is similar to that reported for bulk CFO measured at 300 K ( $M_s$   $\sim 350$  emu cm $^{-3}$ ) [22]. However, the remanent magnetization for CFO bulk ( $M_r$   $\sim 150$  emu cm $^{-3}$ ) is approximately three times the value measured for BLZT–CFO composite thin films ( $M_r$   $\sim 45$  emu cm $^{-3}$ ).

The coupling between the ferroelectric and magnetic orderings was demonstrated by measuring the dielectric polarization hysteresis curve in the presence of a magnetic field, as shown in Fig. 8. The remanent polarization value was reduced from 4.2, 2.2 and 1.8  $\mu\text{C cm}^{-2}$  by increasing the magnetic field from 0.0, 0.6 and 0.8 T, respectively. Similar behaviour has been reported for Bi $_{0.6}$ Tb $_{0.3}$ La $_{0.1}$ FeO $_3$  thin films [23].



Full-size image (46K)

Fig. 8. (a) Dielectric polarization as a function of electric field for a BLZT–CFO thin film measured in magnetic fields of 0.6 and 0.8 T. (b) The ferroelectric remanent polarization ( $P_r$ )

of BLZT–CFO films at room temperature as a function of magnetic field.

#### 4. Conclusions

Nanostructured BLZT–CFO composite thin films were prepared on Nb:STO and Pt substrates by using the rf-magnetron sputtering technique. The films were obtained from  $\text{Ba}_{0.90}\text{La}_{0.067}\text{Zr}_{0.09}\text{Ti}_{0.91}\text{O}_3\text{--CoFe}_2\text{O}_4$  mixed target in a high oxygen-pressure atmosphere. The thin films showed hetero-epitaxial growth and were composed of randomly dispersed CFO nanopillars in the BLZT matrix. XPS studies in depth profile mode confirmed the elemental composition of the film, but was different from  $\text{BaTiO}_3$  in chemical titanium environment. The film exhibited both polarization and magnetization hystereses at room temperature. The magnetoelectric nature of the composite also was demonstrated through the reduction of measured ferroelectric polarization with the application of an external magnetic field.

#### Acknowledgments

This research was supported by the Ministry of Education and Science of Spain through the MAT 2007-63445 project; the Excellence Centre for Novel Materials under Colciencias contract 043-2005; and Colciencias contract 1101-0617622. C. Ostos thanks the Coimbra Group and University of Barcelona for the research grant. The authors gratefully acknowledge the technical support provided by the *Serveis Científico-Técnicos* of the University of Barcelona. Work at WVU was funded through the WVNano Initiative and the National Science Foundation (grant # EPS-0314742).

#### References

- [1] T.P. Ma and J. Han, *IEEE Electron. Device Lett.* **23** (2002), p. 7.
- [2] J.F. Scott and C.A. Paz de Araujo, *Science* **246** (1989), p. 1400.
- [3] K. Maruyama, M. Kondo, S.K. Singh and H.

Ishiwara, *FUJITSU Sci. Tech. J.* **43** (4) (2007), p. 502. [View Record in Scopus](#) | [Cited By in Scopus](#) (2)

[4] J.S. Bunch, A.M. van der Zande, S.S. Verbridge, I.W. Frank, D.M. Tanenbaum, J.M. Parpia, H.G. Craighead and P.L. McEuen, *Science* **315** (2007), p. 954.

[5] S. Matichyn, Ph.D. Thesis, Otto-von-Guericke-Universität Magdeburg, Germany, 2006.

[6] O. Auciello, J.F. Scott and R. Ramesh, *Phys. Today* **51** (1998), p. 22. [Full Text via CrossRef](#) | [View Record in Scopus](#) | [Cited By in Scopus](#) (482)

[7] C. Ostos, M.L. Martínez-Sarrión, L. Mestres, A. Cortes, E. Delgado and P. Prieto, *Braz. J. Phys.* **36** (2006), p. 1062. [View Record in Scopus](#) | [Cited By in Scopus](#) (0)


[8] E. Delgado, C. Ostos, M.L. Martínez-Sarrión, L. Mestres and P. Prieto, *Phys. Status Solidi C* **4** (11) (2007), p. 4099. [Full Text via CrossRef](#) | [View Record in Scopus](#) | [Cited By in Scopus](#) (0)

[9] H. Coufal, L. Dhar and C.D. Mee, *MRS Bull.* **31** (5) (2006), p. 374.

[10] A. Fert and I.A. Campbell, *Phys. Rev. Lett.* **21** (1968), p. 1190. [Full Text via CrossRef](#) | [View Record in Scopus](#) | [Cited By in Scopus](#) (31)

[11] K. Mika and P. Grünberg, *Phys. Rev. Lett.* **57** (1986), p. 2442.

[12] G. Binasch, P. Grünberg, F. Saurenbach and W. Zinn, *Phys. Rev. B* **39** (1989), p. 4828. [Full Text via CrossRef](#) | [View Record in Scopus](#) | [Cited By in Scopus](#) (859)

[13] J.M. Daughton, *Thin Solid Films* **216** (1) (1992), p. 162. [Abstract](#) |  [PDF \(1034 K\)](#) | [View Record in Scopus](#) | [Cited By in Scopus](#) (94)

[14] D.D. Tang, P.K. Wang, V.S. Speriosu, S. Le and K.K. Kung, *IEEE Trans. Magn.* **31** (1995), p. 3206. [Full Text via CrossRef](#) | [View Record in Scopus](#) | [Cited By in Scopus](#) (73)

[15] T.M. Maffitt, J.K. DeBrosse, J.A. Gabric, E.T. Gow, M.C. Lamorey, J.S. Parenteau, D.R. Willmott, M.A. Wood and W.J. Gallagher, *IBM J. Res. Dev.* **50** (1) (2006), p. 25. [View Record in Scopus](#) | [Cited By in Scopus \(10\)](#)

[16] W. Eerenstein, N.D. Mathur and J.F. Scott, *Nature* **442** (2006), p. 759. [Full Text via CrossRef](#) | [View Record in Scopus](#) | [Cited By in Scopus \(324\)](#)

[17] H. Zheng, J. Wang, S.E. Lofland, Z. Ma, L. Mohaddes-Ardabili, T. Zhao, L. Salamanca-Riba, S.R. Shinde, S.B. Ogale, F. Bai, D. Viehland, Y. Jia, D.G. Schlom, M. Wuttig, A. Roytburd and R. Ramesh, *Science* **303** (2004), p. 661. [Full Text via CrossRef](#) | [View Record in Scopus](#) | [Cited By in Scopus \(328\)](#)

[18] K.S. Hwang, T. Manabe, T. Nagahama, I. Yamaguchi, T. Kumagai and S. Mizuta, *J. Cryst. Growth* **237** (2002), p. 464.


[19] W. Gong, J. Li, X. Chu, Z. Gui and L. Li, *Appl. Phys. Lett.* **85** (2004), p. 17.

[20] Q. Li, J. Yin, C. Xiao and Z. Liu, *J. Phys. D: Appl. Phys.* **33** (2000), p. 107. [Full Text via CrossRef](#) | [View Record in Scopus](#) | [Cited By in Scopus \(6\)](#)

[21] C. Ostos, M.L. Martínez-Sarrión, L. Mestres, J.E. García, A. Albareda, R. Perez, *Solid State Sci.*, 2008, in press.

[22] A. Manivannan, A.M. Constantinescu and M.S. Seehra, *Mater. Res. Soc. Symp. Proc.* **658** (2001) GG6.32.1.

[23] V.R. Palkar, K.G. Kumara and S.K. Malik, *Appl. Phys. Lett.* **84** (2004), p. 2856. [Full Text via CrossRef](#) | [View Record in Scopus](#) | [Cited By in Scopus \(24\)](#)

 Corresponding author. Tel.: +34 93 4021225; fax: +34 93 4907725.

[Home](#) [Browse](#) [Search](#) [My Settings](#) [Alerts](#) [Help](#)

---



[About ScienceDirect](#) | [Contact Us](#) | [Information for Advertisers](#) | [Terms & Conditions](#) | [Privacy Policy](#)

Copyright © 2009 Elsevier B.V. All rights reserved. ScienceDirect® is a registered trademark of Elsevier B.V.